Electronic Supplementary Material (ESI) for Nanoscale. This journal is © The Royal Society of Chemistry 2025

Supporting Information

S. aromaticum aqueous extract derived carbon dots: A biosafe antibacterial nanocatalyst for water remediation

Anurag Kumar Pandey[ab], Sayan Mukherjee[c], Nantu Dogra[c], Tapan Kumar Nath[d], Sagar Pal[e], Santanu Dhara[c]*

[a] Department of Electronics and Communication Engineering, Madanapalle Institute of Technology & Science (MITS), Deemed to be University, Madanapalle, Andhra Pradesh 517325, India

[b] School of Nano Science and Technology, Indian Institute of Technology Kharagpur, Kharagpur, West Bengal 721302, India

[c] School of Medical Science and Technology, Indian Institute of Technology Kharagpur, Kharagpur, West Bengal 721302, India

[d] Department of Physics, Indian Institute of Technology Kharagpur, Kharagpur, West Bengal 721302, India

[e] Department of Chemistry, Indian Institute of Technology (ISM) Dhanbad, Jharkhand, India

[*] Corresponding author

Prof. Santanu Dhara (Professor) School of Medical Science and Technology IIT Kharagpur 721302, West Bengal., India
Email: sdhara@smst.iitkgp.ac.in Phone: +91-3222-282306

Total phenols and flavonoids

Bioactive components such as phenols and flavonoids were tested in filtered water-soluble clove extract (CE) and clove extract-derived carbon dots (CECDs) which indicates that the carbonization of clove extract resulted in a decrease of phenolic and flavonoid components. The study shows that water-dispersed and filtered clove extract-derived carbon dots have lower phenolic and flavonoid components compared to un-carbonized clove extract.

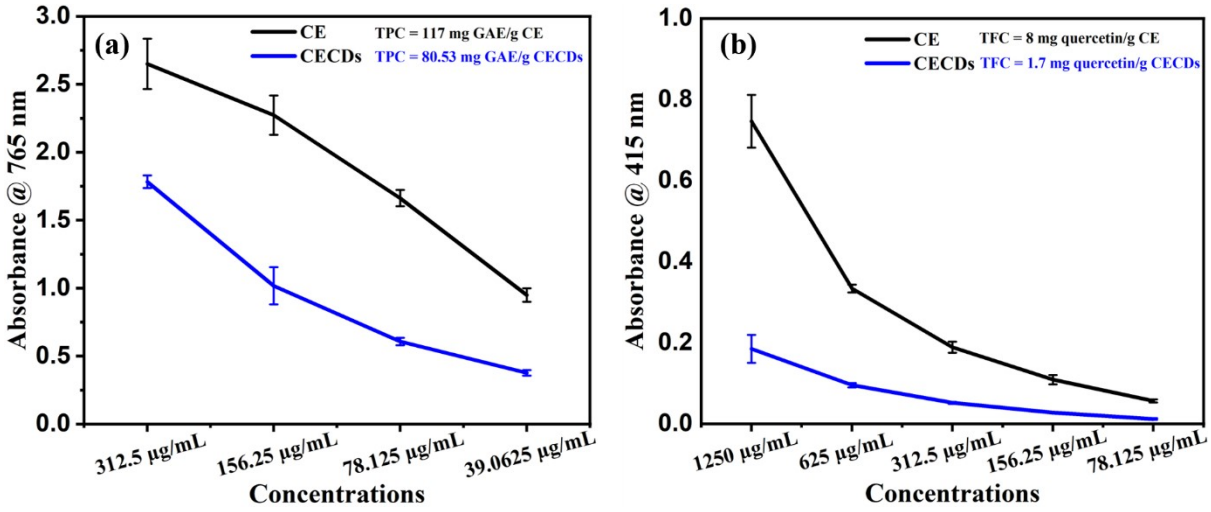

Fig. S.1 (a) Total phenolic component (gallic acid equivalent/g) and (b) total flavonoid component (quercetin equivalent/g) components screening of clove extract (CE) and clove extract derived carbon dots (CECDs).

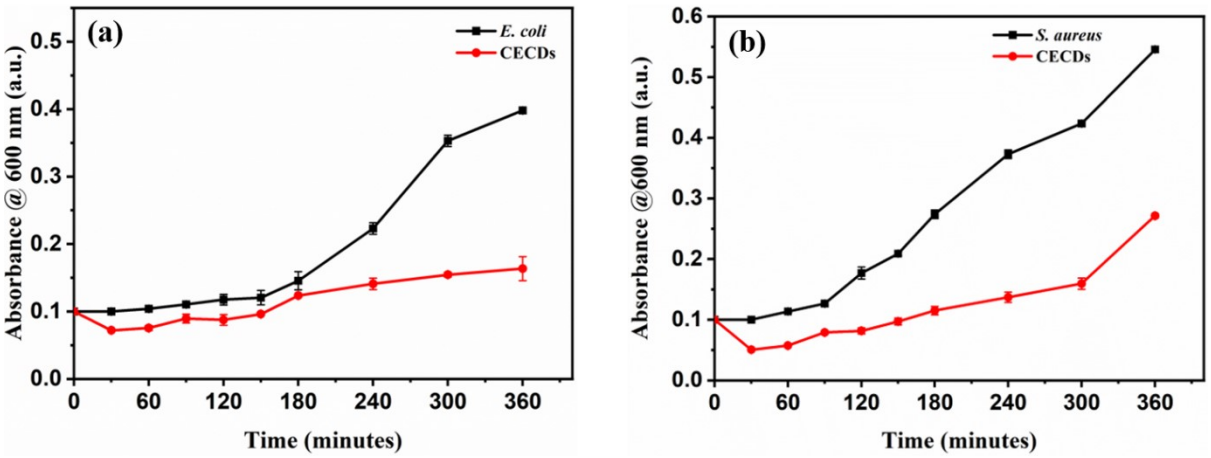

Fig S.2 Growth kinetic curve of (a*) E. coli* and (b) *S. aureus* with and without CECDs (at concentration 1mg/mL). Data are presented as mean ± SD (*n* = 3).

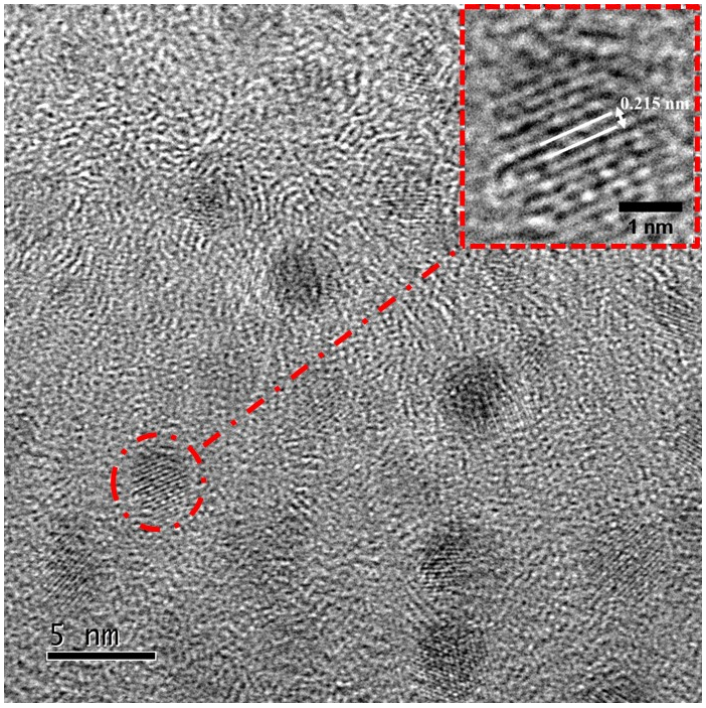

Fig. S3. HRTEM image of CECDs showing clear lattice fringes with an interlayer spacing of ~0.215 nm, indicating graphitic domains within the carbon dots.

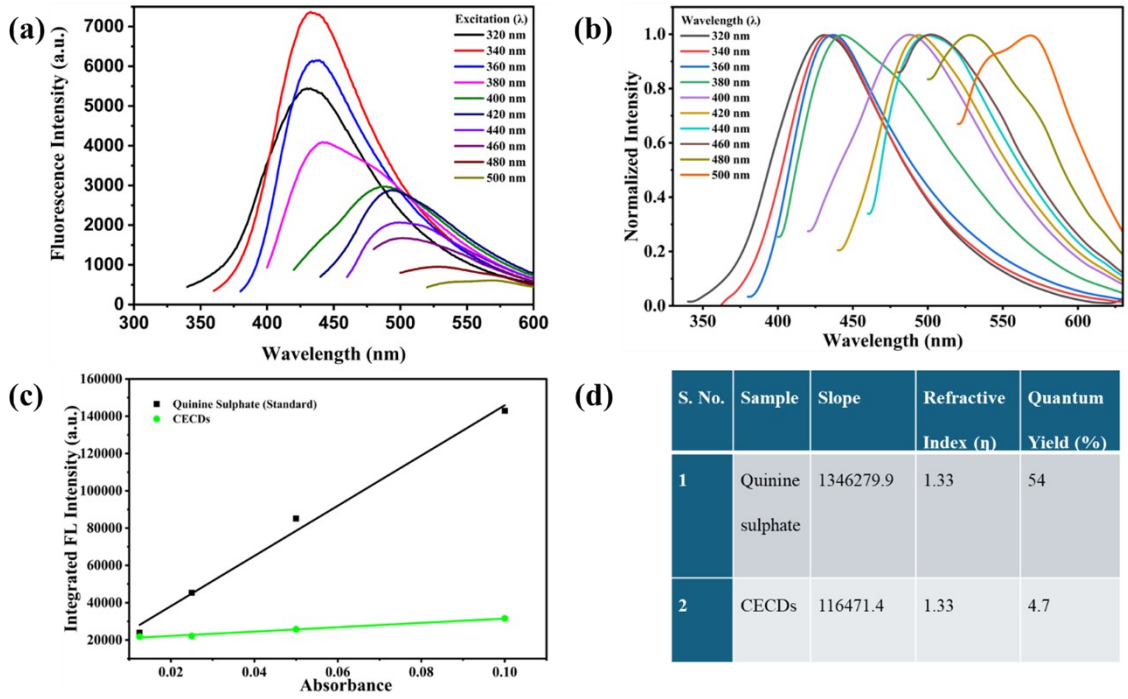

S. No.	Sample	Slope	Refractive Index (η)	Quantum Yield (%)
1	Quinine sulphate	1346279.9	1.33	54
2	CECDs	116471.4	1.33	4.7

Fig S.4 Excitation dependent fluorescence emission spectra (a), normalized fluorescence emission spectra (b) of CECDs by varying the excitation wavelength in the range of 320-500 nm. (c) Quantum yield plot and (d) QY calculation of CECDs (slope) considering quinine sulphate as standard.

PL behaviour of CECDs -The photophysical analysis of CECDs was performed to understand its optical properties. **Fig. S.3 (a)** indicates fluorescence study of CECDs, revealed a excitation dependent fluorescence emissions behaviour by varying the excitation wavelength in the range of 320-500 nm with a 20 nm increment. The CECDs attained their maxima emission at 433 nm and 435 nm while excited at 340 nm and 360 nm excitation wavelengths, respectively. The excitation wavelength-dependent emission behavior of CDs is an outcome of the various surface emissive traps with different energy levels at different wavelengths as represented in **Fig S.3 (b)**. Furthermore, the QY of CECDs were plotted and calculated by considering quinine sulphate as standard, and found to be 4.7% as shown in **Fig. S3 (c, d)**.

Quantum yield (QY)- The QY is the ratio of photons absorbed to photons emitted, which helps to determine the comparative yield of the desired sample (CDs) with respect to a standard sample. The quinine sulphate was used as a standard sample in the experiment. The QY of PPCCDs and CCDs was calculated using the following equation:

$$\textbf{Quantum Yield (QY)} = \mathbf{QY_R} \times \frac{I}{I_R} \times \frac{A_R}{A} \times \frac{n}{n_R}$$

Where A and A_R belong to absorbance, I and I_R are integrated emission intensities, n and n_R are the refractive indexes of the solvent used for both CDs and reference, and QY_R refers to the quantum yield of standard quinine sulphate. The QY plot and calculation of the QY of CECDs was obtained shows 4.7% yield.

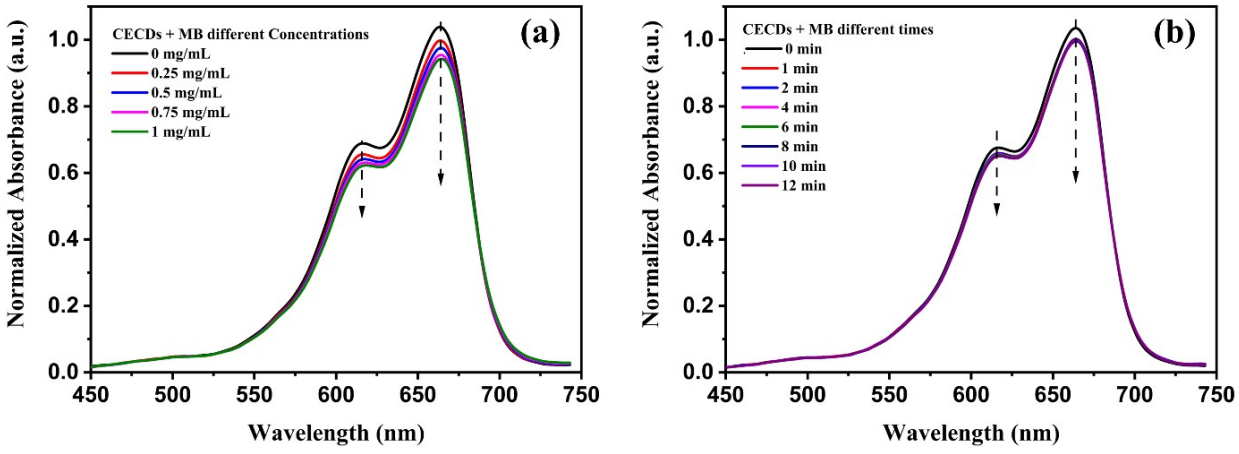

Fig S.5 UV-Visible absorption of (a) MB+CECDs at different concentrations and (b) CECDs + MB at different times by fixing CECDs concentration of 0.5 mg/mL.

Bacterial Membrane Permeability Assay

The permeabilizing impact of the examined nanoparticles on bacterial membranes was assessed using the chromogenic indicators that can be dealt with bacterial enzymes when permitted to pass through specific bacterial regions. Bacterial strains which lacks lactose permeases, constitutively synthesizes cytoplasmic β-galactosidase. Only if the membrane is damaged, the chromogenic substrates for this enzyme penetrate the inner bacterial membranes; so, the conversion to colorful products indicates both the kinetics and degree of membrane damage. When the enzyme is freely available, the marker changes to produce colored products according to normal enzyme kinetics. Utilizing ONPG broth (o-nitrophenyl-β-D-galactoside, Himedia), a substrate for cytoplasmic β-galactosidase we have performed this membrane permeability assay.

A strain of *E. coli* and *S aureus* grown in LB to mid log phase (OD 600 = 0.5) overnight. A volume of 1.0 mL of the culture was placed in Eppendorf tubes, and the suspension was centrifuged at 2500g at r.t. for 10 min. Two times with 1.0 mL of PBS, the resultant cell pellet was washed. Resuspended in 2.0 mL of the ONPG broth, 200 µL of this suspension were put to a well of 96-well plate to get solution with OD420 0.25. Measuring every 30 minutes for 180 minutes and every 60 minutes up to 300 minutes at 37 °C, the increase in absorbance at 420 nm caused by hydrolysis of ONPG inside the cell was recorded. One utilized a control from DI water without chemicals. Three independent trials of o-nitrophenyl produce the values, which show a yellow color visible at 420 nm.

Detection of ROS generation

The level of ROS was investigated using the oxidant-sensing probe 2′,7′-dichlorodihydrofluorescein diacetate (H2DCFDA). After exposure to minimum and maximum concentrations of WCND-DHFI, *E. coli and S. aureus* cells were washed with PBS and subsequently stained with 1 µg/mL H2DCFDA for 1 h. The level of ROS was analyzed using a Thermo Scientific Varioskan LUX platte reader at 488 nm laser (FITC channel).

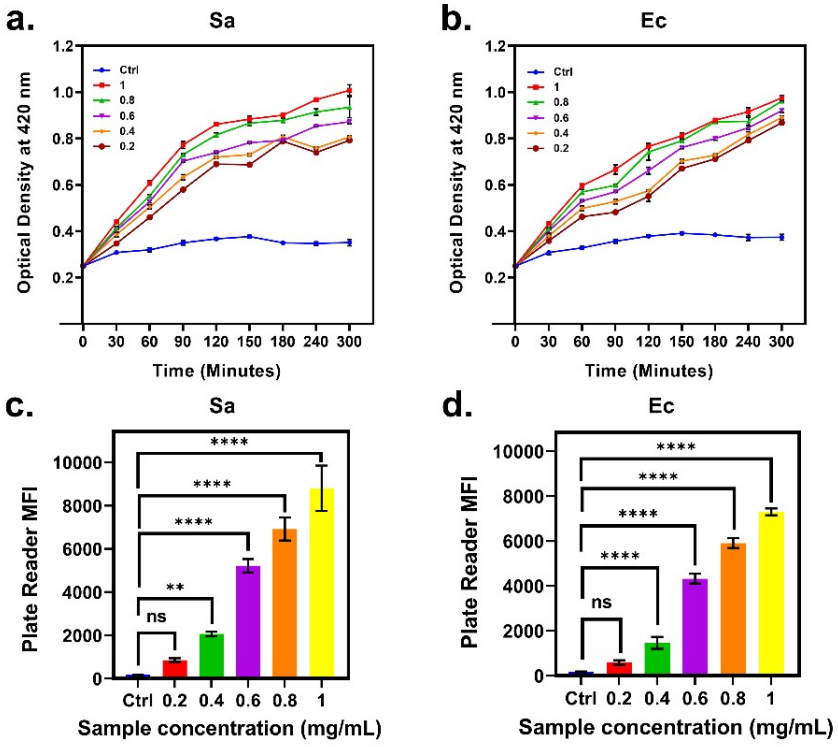

Fig S.6. a-b) Mechanistic Elucidation via ONPG Permeability Assay. *S. aureus* demonstrates a sharp, dose-dependent increase in optical density at 420 nm, whereas *E. coli* shows a similar trend but with a notably lower magnitude of response. c-d) Assessment of ROS generation, reveals a consistent dose-dependent increase in MFI for both strains validating the antibacterial mechanism of CECDs through the induction of oxidative stress through the generation of reactive oxygen species (ROS).

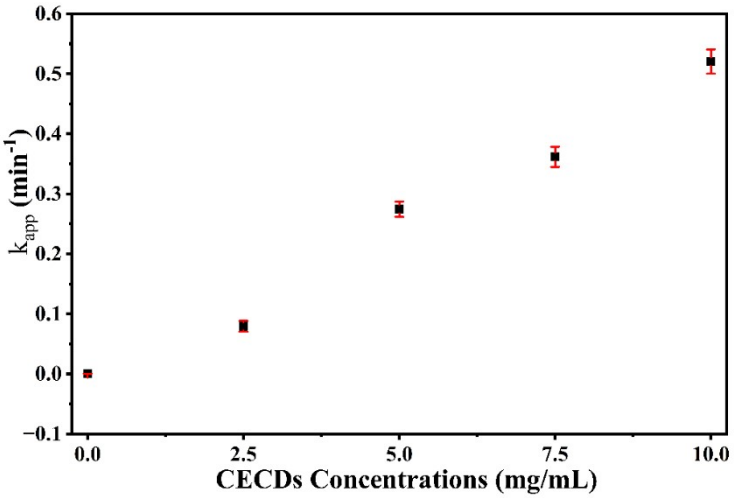

Fig. S7. Error bars represent the standard error of the slope obtained from linear regression of ln(C_0/C) versus time plots.

Table S1: The degradation efficiencies and apparent rate constants (kapp) for each dye

Sl. No	DYE	Degradation (%)	K_{app} (min^{-1})
1.	Methylene Blue (MB)	95.15	0.347 ± 0.012
2.	Rhodamine-B (Rh-B)	22.5	0.0285 ± 0.00123
3.	p-Nitrophenol (pNP)	0.62	0.0013 ± 0.0009

The degradation data clearly demonstrate a strong selectivity toward MB, which exhibits 95.15% removal and a significantly higher rate constant (k_{app} = 0.347 ± 0.012 min^{-1}) compared to Rh-B (22.5%, 0.0285 ± 0.00123 min^{-1}) and pNP (0.62%, 0.0013 ± 0.0009 min^{-1}). The preferential degradation of MB might be arisen from its stronger adsorption on the CECD surface due to electrostatic and π–π interactions, along with more favorable electron transfer kinetics. In contrast, Rh-B experiences steric hindrance, while pNP shows weak adsorption due to electrostatic repulsion under reaction conditions. Additionally, competitive adsorption in the mixed system allows MB to dominate active sites, resulting in significantly higher degradation efficiency."

References:

1. Baker, S. and Baker, G. (2010), Luminescent Carbon Nanodots: Emergent Nanolights. Angewandte Chemie International Edition, 49: 6726-6744. https://doi.org/10.1002/anie.200906623